

Tripodal exTTF-CTV Hosts for Fullerenes

Elisa Huerta,[†] Helena Isla,[‡] Emilio M. Pérez,^{‡,§} Carles Bo,[†] Nazario Martín,^{*,†,§} and Javier de Mendoza^{*,†}

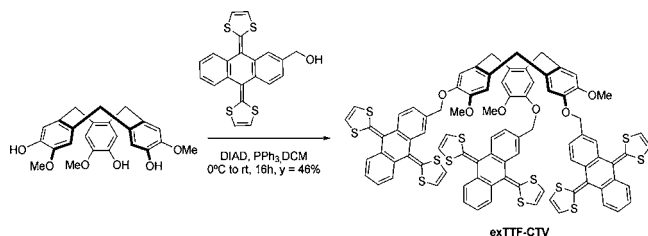
Institute of Chemical Research of Catalonia (ICIQ), Av. Països Catalans, 16, 43007 Tarragona, Spain,
Departamento de Química Orgánica, Facultad de Química, Universidad Complutense, 28040 Madrid, Spain, and
IMDEA-nanociencia, 28049 Madrid, Spain

Received January 26, 2010; E-mail: nazmar@quim.ucm.es; jmendoza@iciq.es

Since the early 1990s, cyclotrimeratrylene (CTV) derivatives have been shown to form “ball and socket” complexes with C₆₀.¹ Recently, some of us have reported hydrogen-bonded self-assembled capsules that associate higher fullerenes (C₇₀ and C₈₄) with increased affinity and selectivity over C₆₀.² In our capsules, two CTV scaffolds endowed with three 2-ureido-4[1*H*]-pyrimidinone subunits self-assemble into dimeric capsules in the presence of the appropriate fullerene host and can be used to purify C₇₀ and C₈₄^{2c} from complex fullerene mixtures (fullerites) without chromatography. Although other receptors for fullerenes based on calixarenes,³ calixpyrroles,⁴ corannulenes,⁵ or tribenzotriquinacenes⁶ have been employed as scaffolds, relatively few examples of hosts in which CTV is combined with other recognition motifs have been reported.⁷ On the other hand, we have reported that the concave aromatic surface of 2-[9-(1,3-dithiol-2-ylidene)anthracen-10(9*H*)-ylidene]-1,3-dithiole (exTTF) can be exploited for the molecular recognition of C₆₀. Even with relatively simple tweezer-like designs, the exTTF-based receptors form complexes with C₆₀ with a binding constant of log *K*_a = 3.5 in chlorobenzene at room temperature.⁸ Later, we have optimized the design of our exTTF-based receptors by making use of bis-exTTF macrocyclic structures, to achieve an improvement of 3 orders of magnitude in the binding constants.⁹

We reasoned an alternative strategy to obtain efficient exTTF-based receptors for fullerenes would be to increase the number of exTTF units in the host. Considering the precedents outlined above, we designed and synthesized host exTTF-CTV, in which three exTTF subunits are linked to a CTV scaffold through short ether linkages. The concave surfaces of both the CTV and the exTTF subunits should nicely wrap around the entrapped fullerene guest. The exTTF-CTV host was readily synthesized from known fragments *via* a simple Mitsunobu coupling (Scheme 1). Its purity and identity were unambiguously established by HPLC-MS, ¹H and ¹³C NMR, and UV–vis.

Scheme 1. Synthesis of exTTF-CTV



An early indication of the ability of exTTF-CTV to bind fullerenes came from the MALDI-TOF spectrum (negative mode,

pyrene matrix). When 1:1 mixtures of exTTF-CTV and either C₆₀ or C₇₀ were analyzed, peaks at *m/z* 2306.3 and 2426.2, corresponding to C₆₀@exTTF-CTV (calcd 2306.1) and C₇₀@exTTF-CTV (calcd 2426.1) respectively were clearly observed. No peaks corresponding to aggregates of other stoichiometries were found. The 1:1 complexes in solution were confirmed by a UV–vis Job’s plot analysis (see the Supporting Information).

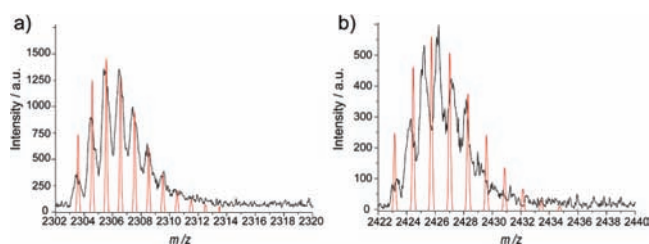


Figure 1. Simulated (red) and found (MALDI-TOF, black) isotopic pattern for (a) C₆₀@exTTF-CTV and (b) C₇₀@exTTF-CTV.

The host shows rather complex ¹H NMR spectra (500 MHz) at room temperature in CDCl₃/CS₂ (2:5 v/v) or in *d*₈-toluene, indicative of the coexistence of several stable conformations in solution, in slow chemical exchange. Indeed, splitting and sharpening of most signals were observed upon cooling, in both solvents. Similarly, heating caused the spectrum to significantly simplify at 378 K in *d*₈-toluene, although without matching with a C₃ symmetric molecule. However, the spectrum displays a single set of broad signals at room temperature in *d*₅-chlorobenzene, which is fully resolved at 353 K. The binding event produced slight, though reproducible changes in the ¹H NMR of exTTF-CTV. Additionally, the C₆₀ ¹³C NMR signal was shifted upfield and broadened in C₆₀@exTTF-CTV, both processes being strengthened upon cooling (see the Supporting Information).

The stability of the complexes was estimated through three independent UV–vis titrations. In a typical experiment, 0.1 equiv aliquots of the fullerene were added (up to 3.3 equiv) to a constant concentration of the exTTF-CTV host (10^{−4} M, chlorobenzene). Upon addition of either C₆₀ or C₇₀ a significant decrease in intensity of the exTTF band at λ_{max} = 434 nm was observed (Figure 2), accompanied by the emergence of an intense charge-transfer band centered at λ = 478 nm for C₆₀ and at λ = 472 nm for C₇₀. During the early steps of the titration (after addition of 1–1.2 equiv of guest), well-defined isosbestic points at 452 nm (C₆₀) and 445 nm (C₇₀) were observed. The changes in the electronic absorption spectra are fully consistent with those found for our previously reported tweezer-like exTTF receptors^{8,9} and constitute the typical signature of the exTTF–fullerene interaction.¹⁰

Analysis of the UV–vis data was carried out with both Specfit and Origin software, in the latter case fitting the data to the equation

[†] Institute of Chemical Research of Catalonia.

[‡] Universidad Complutense.

[§] IMDEA-nanociencia.

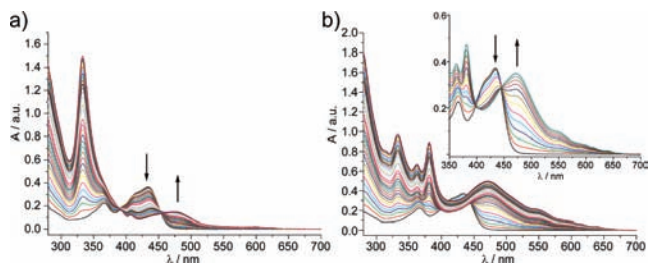


Figure 2. UV-vis spectra as recorded during the titration of (a) **exTTF-CTV** vs C_{60} and (b) **exTTF-CTV** vs C_{70} (inset shows the first 12 additions), PhCl, 298 K.

currently employed by us^{8,9} and by others¹¹ (see the Supporting Information). An association constant toward C_{60} of $\log K_a = 5.3 \pm 0.2$ was obtained. With regard to C_{70} , analysis of the titration data produced a binding constant of $\log K_a = 6.3 \pm 0.6$, 10-fold higher than that found for C_{60} . The values of the binding constants are among the highest reported to date for a nonmetalloporphyrin containing host and comparable to those reported by the groups of Boyd, Reed, and Armaroli for bisporphyrin tweezers^{3a} and by Aida for bisporphyrin cages,¹² with the exception of the Rh(III)^{12b} and Ir(III)^{12c} metalloporphyrin derivatives.

The electrochemical characterization of **exTTF-CTV** and its fullerene complexes was carried out by cyclic voltammetry of 10^{-5} M solutions in chlorobenzene/acetonitrile (5:1 v/v) (0.1 M of Bu_4NClO_4 as electrolyte, glassy carbon as working electrode, Pt wire as counter electrode, Ag/AgCl as reference electrode, scan rates: 25, 50, 100, and 200 mV/s). The voltammogram of **exTTF-CTV** displays the characteristic electrochemically irreversible oxidation of exTTF at 0.36 V, with a weak shoulder at 0.74 V, most probably due to weak adsorption processes. Upon complexation with either fullerene, we observed a significant shift of the oxidation potential to 0.54 V. With respect to the reduction waves of the fullerenes we observed the first four reduction processes for C_{60} , C_{70} , and their complexes. The changes to the first and second reduction potential upon complexation are approximately 10–50 mV, while the third reduction process is affected to a greater extent, up to 100 mV in the case of $C_{70}@exTTF-CTV$.

Table 1. Redox Potentials (V vs Ag/Ag⁺) of **exTTF-CTV**, C_{60} , C_{70} , and Their Complexes

	E^1_{red}	E^2_{red}	E^3_{red}	E^4_{red}	E^1_{ox}
exTTF-CTV	—	—	—	—	0.36
C_{60}	−0.50	−0.92	−1.41	−1.87	—
$C_{60}@exTTF-CTV$	−0.49	−0.91	−1.37	—	0.54
C_{70}	−0.51	−0.92	−1.37	−1.77	—
$C_{70}@exTTF-CTV$	−0.48	−0.87	−1.27	−1.74	0.54

The structure and properties of the complexes were determined computationally by using DFT methods as implemented in the ADF v.2008 package.¹³ Full geometry optimizations were carried at the BP86/DZP level, while final energies were evaluated by single-point calculations at the BP86/TZP and BH&H/TZ2P levels. Despite the intrinsic limitations of pure DFT methods for evaluating nonbonding interaction energies, we found recently that this hybrid method was suitable to evaluate the interaction strength of these species in the gas phase.^{8b,c,9,14} As predicted by our initial modeling, the calculated structures show that the fullerenes dwell deep into the cavity of the **exTTF-CTV** host, with the CTV serving as both a bowl-shaped recognition element and as a preorganizing scaffold for the exTTF subunits, which wrap almost completely around the surface of the fullerenes. Host deformation energies, calculated as

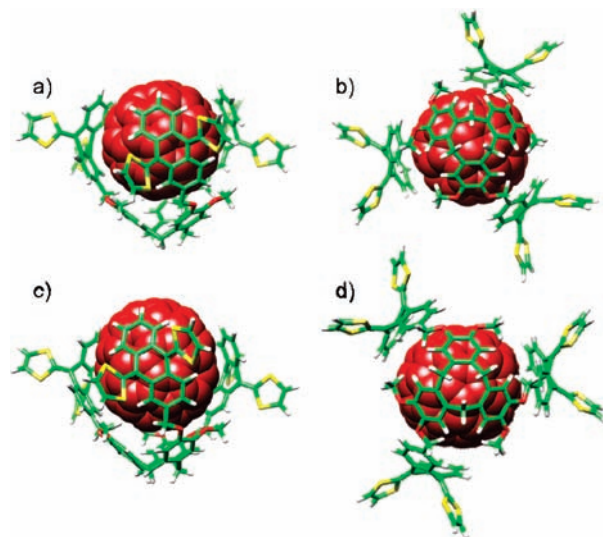


Figure 3. Energy-minimized structures (DFT) of (a) $C_{60}@exTTF-CTV$ side view, (b) $C_{60}@exTTF-CTV$ top view, (c) $C_{70}@exTTF-CTV$ side view, and (d) $C_{70}@exTTF-CTV$ top view.

the difference between the energy of the host in the complex and the energy of the free **exTTF-CTV** structure at both the BP86/TZP and BH&H/TZ2P levels, gave convergent results. **exTTF-CTV** requires 7–9 kcal mol^{−1} to adapt to C_{60} , whereas less deformation, namely 1.5–2.5 kcal mol^{−1}, is needed to form the complex with C_{70} . The average angle between the centroids of two consecutive aromatic rings in the CTV and the linking methylene carbon in the $C_{60}@exTTF-CTV$ complex is 113.6° and slightly larger (114.0°) for $C_{70}@exTTF-CTV$. The curvature of the exTTF units is also dependent on the guest. The average angle between the planes defined by the two aromatic rings of each exTTF subunit is 49.9° for $C_{60}@exTTF-CTV$ and 52.0° for $C_{70}@exTTF-CTV$. The energy release to build up the complex starting from the two isolated units computed at the BH&H level nicely correlates with the binding constants reported above and with those of related systems.^{8,9} For $C_{70}@exTTF-CTV$, the interaction energy is −22.1 kcal mol^{−1}, while for $C_{60}@exTTF-CTV$ we evaluated −15.0 kcal mol^{−1}. These values also agree with the tiny amount of charge transferred from host to the fullerene (0.31 for C_{70} , 0.25 for C_{60}) when forming the complex. TDDFT calculations (BP86, DZP) were carried out to shed light on the electronic absorption spectra. The charge transfer band is quite accurately reproduced by the calculations, with a calculated $\lambda_{max} = 498$ nm (observed = 478 nm) for a C_{60} complex and $\lambda_{max} = 484$ nm (observed = 472 nm) for a C_{70} complex (see the Supporting Information).

Besides the very high binding constants, one of the most significant features of the $C_{60}@exTTF-CTV$ complex is the combination of shape and electronic complementarity between exTTF and C_{60} . We have previously shown that photoinduced electron transfer (PET) from the electron donor exTTF to the electron acceptor C_{60} occurs readily in our tweezer-like receptors.^{8c} This is also the case for the $C_{60}@exTTF-CTV$ complex, as demonstrated by preliminary light-induced electron spin resonance measurements at 298 K (Figure 4). When a 1:1 mixture of C_{60} and **exTTF-CTV** in deaerated PhCl—ESR silent in the dark—was irradiated with a broad-band Hg lamp, a clearly visible, albeit weak signal ($g = 2.0014$; $\Delta H = 5.9$ G) was observed,¹⁵ which increases in intensity with irradiation time and decreases rapidly upon switching the lamp off. To unambiguously establish the PET origin of this ESR signal, control LESR experiments were carried out with

both C_{60} and **exTTF-CTV** separately, which remained ESR silent under light irradiation.

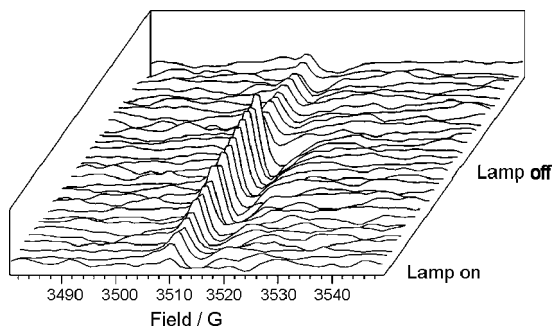


Figure 4. ESR spectra of C_{60} @**exTTF-CTV** (PhCl, 298 K) taken at 45 s intervals. The sample was irradiated with a broad-band Hg lamp.

In summary, **exTTF-CTV** features the combination of two concave recognition fragments, resulting in a very effective association of both C_{60} and C_{70} , with binding constants comparable to the strongest reported in the literature for metalloporphyrin-based receptors, and superior to any other receptors containing only purely organic fragments. Taking into account the successful application of our previous receptors—with binding constants 2 orders of magnitude weaker—to the construction of nanostructured electroactive materials¹⁶ and the relatively simple synthetic route that gives access to **exTTF-CTV**, we will focus our future research on the utilization of this new host—guest system to similar goals. Finally, given the chiral nature of the CTV central scaffold, the enantioselective recognition of the D_2 -isomers of higher fullerenes C_{76} and C_{84} constitutes current pursuit in our laboratories.¹⁷

Acknowledgment. Financial support by MICINN of Spain (projects CTQ2008-00795/BQU, CTQ2006-14987-C02-02/BQU, CSD2007-00010, CTQ2005-08948, CTQ2008-00183, and Consolider Ingenio 2010 CSD 2006-0003), the ESF (SOHYD MAT2006-28170-E), the ICIQ Foundation, the CAM (MADRISOLAR-2 S2009/PPQ-1533), and European FEDER funds is acknowledged. E.H., H.I., and E.M.P. thank the MICINN for an FPI, an FPU studentship, and a Ramón y Cajal fellowship, cofinanced by the European Social Fund, respectively.

Supporting Information Available: Supplementary figures, experimental and computational details. This material is available free of charge via the Internet at <http://pubs.acs.org>.

References

- Steed, J. W.; Junk, P. C.; Atwood, J. L.; Barnes, M. J.; Raston, C. L.; Burkhalter, R. S. *J. Am. Chem. Soc.* **1994**, *116*, 10346.
- (a) Huerta, E.; Metselaar, G. A.; Fragoso, A.; Santos, E.; Bo, C.; de Mendoza, J. *Angew. Chem., Int. Ed.* **2007**, *46*, 202. (b) Huerta, E.; Cequier, E.; de Mendoza, J. *Chem. Commun.* **2007**, 5016. (c) Mendoza, J. D.; Huerta Martinez, E.; Metselaar, G.; Institut Catala D'Investigacio Quimica, Spain; Application: US, 2008; 20 pp.
- (a) Hosseini, A.; Taylor, S.; Accorsi, G.; Armaroli, N.; Reed, C. A.; Boyd, P. D. W. *J. Am. Chem. Soc.* **2006**, *128*, 15903. (b) Atwood, J. L.; Barbour, L. J.; Nichols, P. J.; Raston, C. L.; Sandoval, C. A. *Chem.—Eur. J.* **1999**, *5*, 990.
- (a) Nielsen, K. A.; Martin-Gomis, L.; Sarova, G. H.; Sanguinet, L.; Gross, D. E.; Fernández-Lazaro, F.; Stein, P. C.; Levillain, E.; Sessler, J. L.; Guldi, D. M.; Sastre-Santos, A.; Jeppesen, J. O. *Tetrahedron* **2008**, *64*, 8449. (b) Nielsen, K. A.; Sarova, G. H.; Martin-Gomis, L.; Fernández-Lazaro, F.; Stein, P. C.; Sanguinet, L.; Levillain, E.; Sessler, J. L.; Guldi, D. M.; Sastre-Santos, A.; Jeppesen, J. O. *J. Am. Chem. Soc.* **2008**, *130*, 460.
- (a) Mizyed, S.; Georghiou, P.; Bancu, M.; Cuadra, B.; Rai, A. K.; Cheng, P.; Scott, L. T. *J. Am. Chem. Soc.* **2001**, *123*, 12770. (b) Georghiou, P. E.; Tran, A. H.; Mizyed, S.; Bancu, M.; Scott, L. T. *J. Org. Chem.* **2005**, *70*, 6158.
- Georghiou, P. E.; Dawe, L. N.; Tran, H.-A.; Strube, J.; Neumann, B.; Stammer, H.-G.; Kuck, D. *J. Org. Chem.* **2008**, *73*, 9040.
- (a) Matsubara, H.; Shimura, T.; Hasegawa, A.; Semba, M.; Asano, K.; Yamamoto, K. *Chem. Lett.* **1998**, 1099. (b) Nierengarten, J.-F. *Fullerenes, Nanotubes, Carbon Nanostruct.* **2005**, *13*, 229. (c) Hardie, M. J.; Godfrey, P. D.; Raston, C. L. *Chem.—Eur. J.* **1999**, *5*, 1828.
- (a) Pérez, E. M.; Sánchez, L.; Fernández, G.; Martín, N. *J. Am. Chem. Soc.* **2006**, *128*, 7172. (b) Pérez, E. M.; Capodilupo, A. L.; Fernández, G.; Sánchez, L.; Viruela, P. M.; Viruela, R.; Ortí, E.; Bietti, M.; Martín, N. *Chem. Commun.* **2008**, 4567. (c) Gayathri, S. S.; Wielopolski, M.; Pérez, E. M.; Fernández, G.; Sánchez, L.; Viruela, R.; Ortí, E.; Guldi, D. M.; Martín, N. *Angew. Chem., Int. Ed.* **2009**, *48*, 815. (d) Pérez, E. M.; Martín, N. *Chem. Soc. Rev.* **2008**, *37*, 1512.
- Isla, H.; Gallego, M.; Pérez, E. M.; Viruela, R.; Ortí, E.; Martín, N. *J. Am. Chem. Soc.* **2010**, *132*, 1772.
- In fact, these changes correspond to the (partial) formation of the **exTTF** radical cation; see: (a) Jones, A. E.; Christensen, C. A.; Perepichka, D. F.; Batsanov, A. S.; Beeby, A.; Low, P. J.; Bryce, M. R.; Parker, A. W. *Chem.—Eur. J.* **2001**, *7*, 973. (b) Guldi, D. M.; Sánchez, L.; Martín, N. *J. Phys. Chem. B* **2001**, *105*, 7139.
- Schalley, C. Editor *Analytical Methods in Supramolecular Chemistry*, 2007.
- (a) Tashiro, K.; Aida, T. *Chem. Soc. Rev.* **2007**, *36*, 189–197. (b) Zheng, J.-Y.; Tashiro, K.; Hirabayashi, Y.; Kinbara, K.; Saigo, K.; Aida, T.; Sakamoto, S.; Yamaguchi, K. *Angew. Chem., Int. Ed.* **2001**, *40*, 1857. (c) Yanagisawa, M.; Tashiro, K.; Yamasaki, M.; Aida, T. *J. Am. Chem. Soc.* **2007**, *129*, 11912.
- (a) Baerends, E. J.; Ellis, D. E.; Ros, P. *Chem. Phys.* **1973**, *2*, 41. (b) Baerends, E. J.; Ros, P. *Chem. Phys.* **1973**, *2*, 52. (c) Guerra, C. F.; Suijders, J. G.; Te Velde, G.; Baerends, E. J. *Theor. Chem. Acc.* **1998**, *99*, 391. (d) Te Velde, G.; Baerends, E. J. *J. Comput. Phys.* **1992**, *99*, 84. (e) Boerigter, P. M.; Te Velde, G.; Baerends, E. J. *Int. J. Quantum Chem.* **1988**, *33*, 87. (f) Vosko, S. H.; Wilk, L.; Nusair, M. *Can. J. Phys.* **1980**, *58*, 1200. (g) Becke, A. D. *Phys. Rev. A* **1986**, *33*, 2786. (h) Becke, A. D. *Phys. Rev. A* **1988**, *38*, 3098. (i) Levy, M.; Perdew, J. P. *J. Chem. Phys.* **1986**, *84*, 4519.
- For a comprehensive comparative study of the performance of different DFT functionals for the evaluation of supramolecular systems, see: Zhao, Y.; Truhlar, D. G. *J. Chem. Theory Comput.* **2007**, *3*, 289. The authors demonstrate that BH&H is reliable for systems dominated by dispersion interactions, such as ours.
- Unambiguous assignment of this signal is not straightforward. It can be attributed to the photogenerated $C_{60}^{\cdot-}$ encapsulated in the **exTTF-CTV** receptor: the free $C_{60}^{\cdot-}$ shows an ESR signal with $g = 1.9984$ and $\Delta H = 30.9$ G at 213 K. Both the increase in g value and the decrease in ΔH correspond to a lowering of the symmetry of $C_{60}^{\cdot-}$, as would be the case in $C_{60}^{\cdot+}$ @**exTTF-CTV** (see: Fukuzumi, S.; Mori, H.; Suenobu, T.; Gao, X.; Kadish, K. M. *J. Phys. Chem. A* **2000**, *104*, 10688). Alternatively, it could also be due to **exTTF**⁺ since similar compounds show ESR signals with $g = 2.0028$ – 2.0034 (Perepichka, D. M.; Bryce, M. R.; Perepichka, I. F.; Lyubchik, S. B.; Christensen, C. A.; Godbert, N.; Batsanov, A. S.; Levillain, E.; McInnes, E. J. L.; Zhao, J. P. *J. Am. Chem. Soc.* **2002**, *124*, 14227). Most probably, it is due to the overlap of both signals.
- For recent reviews on the supramolecular chemistry of TTF derivatives, see: (a) Canevet, D.; Salle, M.; Zhang, G.; Zhang, D.; Zhu, D. *Chem. Commun.* **2009**, 2245. (b) Pérez, E. M.; Illescas, B. M.; Herranz, M. A.; Martín, N. *New J. Chem.* **2009**, *33*, 228. For examples of self-organized electroactive materials comprising **exTTF** and C_{60} derivatives, see: (c) Fernández, G.; Sánchez, L.; Pérez, E. M.; Martín, N. *J. Am. Chem. Soc.* **2008**, *130*, 10674. (d) Fernández, G.; Pérez, E. M.; Sánchez, L.; Martín, N. *J. Am. Chem. Soc.* **2008**, *130*, 2410. (e) Fernández, G.; Pérez, E. M.; Sánchez, L.; Martín, N. *Angew. Chem., Int. Ed.* **2008**, *47*, 1094.
- For an example of enantioselective sensing of chiral fullerenes, see: Shoji, Y.; Tashiro, K.; Aida, T. *J. Am. Chem. Soc.* **2006**, *128*, 10690.

JA1006993